The Abdus Salam
International Centre for Theoretical Physics

United Nations
Educational, Scientific and
Cultural Organization

IAEA
International Atomic Energy Agency

2016-2

Joint ICTP/IAEA Advanced Workshop on Earthquake Engineering for Nuclear Facilities

30 November - 4 December, 2009

Implementing SSHAC level 4 PSHA results into a plant specific PSA the case of PEGASOS

Jens-Uwe Klügel

Kernkraftwerk Goesgen-Daeniken
Daeniken
Switzerland

Joint ICTP/IAEA Advanced Workshop on Earthquake Engineering for Nuclear Facilities

30 November- 4 December 2009

Implementing SSHAC level 4 PSHA results into a plant specific PSA – the case of PEGASOS

Dr. Jens-Uwe Klügel
Kernkraftwerk Goesgen-Daeniken, Kraftwerkstrasse, 4658 Daeniken, Switzerland

Member of the Seismological Society of America

Implementing SSHAC level 4 PSHA results into a plant specific PSA – the case of PEGASOS

Dr. Jens-Uwe Klügel

Kernkraftwerk Goesgen-Daeniken, Kraftwerkstrasse, 4658 Daeniken, Switzerland

ABSTRACT: From 2000 to 2004 the Swiss nuclear power plants were requested by the regulatory authority to sponsor the PEGASOS project – a large-scale SSHAC level 4 probabilistic seismic hazard analysis (PSHA) with broad involvement of international experts. The results of this study had to be implemented into the plant-specific seismic PSA (Probabilistic Safety Analysis). The lecture gives an overview on the problems encountered and the methods used leading to n successful implementation of the PEGASOS results. Finally, the main results of the updated plant specific PSA are discussed, showing the large contribution of seismic events to the overall risk of a nuclear power plant.

1 Introduction

The NPP Goesgen has completed its first plant specific PSA (level 1= evaluation of core and fuel damage frequency, and level 2 = evaluation of radioactivity release frequencies and the associated source terms) in 1994. The study included all (feasible at the site) internal and external events including a seismic PSA and considered all plant operational modes. Since then the plant specific PSA has been updated several times.

From 2000 to 2004 the Swiss nuclear power plants were requested by the regulatory authority to sponsor the PEGASOS-project (Abrahamson et al, 2004) a large scale SSHAC level 4 PSHA study (SSHAC, 1997) to improve the assessment of seismic risk in support of plant-specific seismic PSAs. The main goal of the project consisted in the development of a more realistic seismic hazard as an input for the seismic PSA with the main focus on a realistic representation of the hazard uncertainties. Earlier PSA studies had shown the large impact of these uncertainties to the overall uncertainties of the PSA results. After completion of the study the Swiss regulatory authority required the implementation of the results into the plant specific seismic PSA.

2 General Methodology of seismic PSA

This section gives a short overview on the main procedural steps required for the development of a seismic PSA. The main focus is given to discuss the link between seismic hazard analysis and the seismic risk evaluation.

2.1 Elements of risk analysis

The key elements of risk analysis (Kaplan & Garrick 1981) as used in the nuclear industry are:

1. Identification of events that can occur and have adverse consequences
2. Estimation of the likelihood of those events occurring
3. Estimation of the potential consequences.

Therefore, the results of a risk analysis can be presented as a set of triplets:

$$R = \langle H_i, P_i, C_i \rangle \qquad \textbf{(1)}$$

H_i represents the set of *i* events with possible adverse consequences

P_i represents the associated probabilities of their occurrence

C_i represents the associated intolerable consequences.

2.2 General procedure of a seismic PSA

In general compliance with the elements of risk analysis described in section 2.1 a seismic PSA consists of the following procedural steps:

1. Development of a probabilistic description of the seismic hazard (in this case the PEGASOS project) – identifying the hazard events H_i and their associated frequencies
2. Developing a detailed fragility analysis resulting in a mathematical description of the failure probability of safety important components, structures and equipment
3. Development of a plant logic model (the risk model) which is a Boolean expression for the interdependency of plant functions and the associated system functions
4. Quantification of the model and uncertainty analysis

This means that a seismic hazard analysis performed in step 1 shall provide the following information as an input for a probabilistic safety assessment (PSA):

- The events which may potentially endanger our infrastructure
- The frequency or probability of occurrence of these events.

The consequences of these events are evaluated by the risk model of the plant, which essentially represents a logic model mapping the hazards to be investigated to their consequences.

2.3 Probabilistic seismic hazard analysis – evaluation of the PEGASOS results

As required by the regulator the results of the PEGASOS project were used as the probabilistic description of the seismic hazard.

The PEGASOS project followed the methodology of the SSHAC (1997) procedures for the treatment of uncertainties including the extensive use of experts at its most elaborate way – level 4 – in conjunction with a logic tree methodology for the quantification of seismic hazard. The project was subdivided into four subprojects:

- Subproject 1 (SP1): Source Characterization
- Subproject 2 (SP2): Ground Motion Characterization
- Subproject 3 (SP3):Site Effect Characterization
- ˜Subproject 4 (SP4) Seismic Hazard Computation

An unprecedented feature of the project was the SSHAC Level-4 treatment of site-specific geological host-ground effects on the character of incoming ground motion to be resisted by structural design features.

A total of 21 well-known experts were nominated as participants in the project. Two other experts, one of them a coauthor of the SSHAC procedures, participated in the project as team facilitators for the expert elicitation process. A very strict quality assurance program was established for the project. Such a program was required because many of the involved organizations and individual experts were not certified according to the ISO requirements.

For the quantification of the seismic hazard the code FRISK88M® was used, which is qualified by US NRC and is based on the use of logic trees, the assumption of a stationary homogenous Poisson process for earthquake recurrence and the truncated Gutenberg-Richter-correlation for describing magnitude recurrence in areal sources. The PEGASOS project led to surprising results. A comparison of the hazard curves and uniform hazard spectra obtained for different exceedance frequencies with comparable hazard estimates for other more seismically active regions as well as with historical seismicity showed an astonishing similarity to seismically more active regions like Turkey, Iran or even to Japan and California (Klügel, 2005a-c). The main results of the study showed an astonishing similarity of the seismic hazard at the Goesgen site with the seismic hazard in countries with a significantly higher exposure to seismic risk. This can be illustrated by presenting some results for the Goesgen site. Figure 1 shows the hazard curves for pga and 5 Hz with and without CAV filtering (see below).

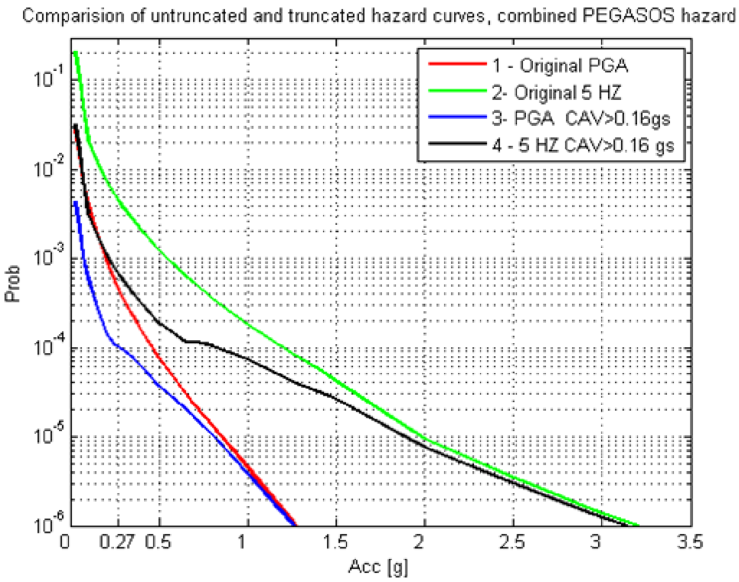

Figure 1 Results of the PEGASOS study for the Goesgen site (with and without CAV filtering), soil hazard

Nevertheless, a more detailed analysis revealed that hazard curves derived from a traditional PSHA are misleading and cannot be used directly for making any meaningful assessment of the seismic risk associated with them. A detailed review of the underlying SSHAC-procedures (Klügel, 2005a, Klügel, 2007a, Klügel 2008a) and their implementation in the PEGASOS study revealed that these surprising results are directly linked to technical and methodological deficiencies in the SSHAC-procedures. The most important issues are:

1. The application of the Ang and Tang model (Ang, 1975, 1984) combining different types of uncertainty – aleatory variability and epistemic uncertainty – into a combined random parameter (Ayyub, 2006). As a side remark it is interesting to note that in the second edition of their book, Ang and Tang (Ang, 2006) dissociate themselves from this concept, emphasizing the different significances of epistemic (lack of knowledge)

uncertainty and aleatory variability (randomness, e.g. variation in a population), which require that they be separately treated mathematically .

2. The use of inconsistent modelling assumptions leading to an incorrect calculation of the probability of exceedance of earthquake ground motion levels (accelerations) (Klügel, 2007a).

3. The possible violation of energy conservation principles caused by summing up exceedance frequency contributions to a certain acceleration level from weak (low energy) earthquakes and from strong earthquakes (Klügel, 2007b). This process is illustrated in figure 2. The figure shows that in the PSHA methodology, exceedance frequencies are added despite the different damaging potentials of the associated earthquakes expressed by an intensity parameter (for example EMS-98 intensity).

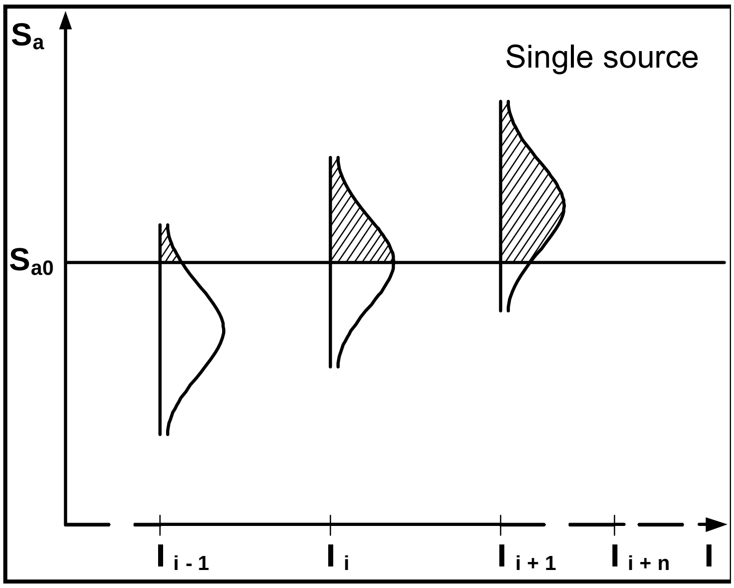

Figure 2 Evaluation of an UHS in traditional PSHA, (single source, I – Intensity (damage index))

Figure 3 shows the consequences of the computational procedure of traditional PSHA analysis with respect to energy considerations. It compares the strong motion duration (uniform duration according to Bolt (1973) in s) of two earthquakes of significantly different magnitudes which result in the same peak ground acceleration at the site of interest (at distance D from the earthquake location). Therefore, the computational procedure of PSHA treats earthquakes of completely different energy content as equally damaging which contradicts empirical evidence obtained from real earthquakes as well as from tests.

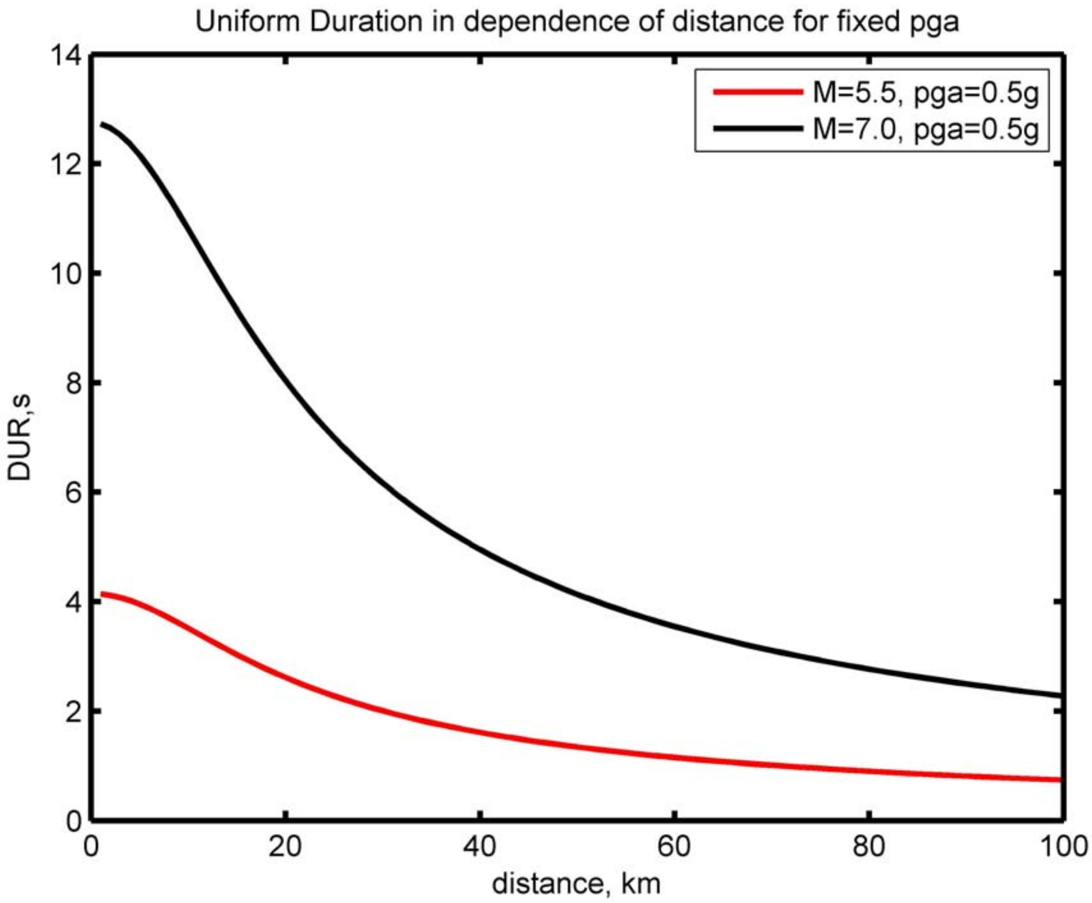

Figure 3 Comparison of the strong motion duration (uniform duration according to Bolt (1973) of earthquakes of different magnitudes (5.5 and 7.0) resulting in the same pga at a site

4. The use of inadequate expert opinion elicitation and aggregation methods (Klügel 2005c, Cooke, 1991, Cooke, 2008) which are based on political consensus principles or on census, rather than on principles of rational consensus.

The failure to consider energy conservation principles has the consequence that the output of a PSHA – the hazard curves or the so-called uniform hazard spectrum - is driven by low energy near-site earthquakes. Such earthquakes do not cause damage even at very high accelerations, as has been shown by an increasing number of observations of high accelerations from small to moderate earthquakes near the sites of nuclear power plants. It was shown (Vanmarcke, 1980) that for a given elastic energy content (expressed by the ARIAS-intensity (Arias, 1970)) the strong motion duration decreases nearly proportionally with the increase of the peak values of peak ground acceleration.

1. The apparent contradiction between the high accelerations observed and lack of damage, although such would have been predicted by current calculation procedures, can be explained by the prevailing use of linear-elastic calculation methods based on response spectra (for example, soil-structure interactions in industrial practice are calculated in the frequency domain, e.g. using the SASSI code). These methods are not capable of correctly accounting for the difference in the energy content of low magnitude and high magnitude events. Neglecting this problem in risk analysis would lead to a significant overestimation of seismic risk, with a possible adverse impact on risk-informed decision making. This poses a strong challenge to risk analysts intending to develop a realistic seismic risk assessment, as is necessary for responsible decision-making in an increasingly risk-informed environment. The most important correction to be made consists in the restoration of energy conservation principles with respect to the PSHA results. There are several possible ways of restoring energy conservation principles in the aftermath of a PSHA: Introduction of an energy threshold, defining the onset of damage for well-designed structures and components.

2. Scaling damage effects to energy measures and implementing correction factors into the fragility analysis.

3. Direct nonlinear dynamic analysis using coupled models of structures and components.

All these possible alternatives require a more detailed knowledge of the true hazard background (compare figure 2). Therefore, the decision was made to perform a detailed disaggregation of the PEGASOS hazard for a better understanding of the real hazard consequences. The disaggregation was performed for rock conditions (FRISK88M® does not include a soil hazard model) for three different distance ranges (D1 <16km, D2 between 16 and 40 km, D3 >40 km up to 250 km) for different spectral accelerations separately for each of the expert opinion combinations and for 4 different hazard exceedance frequencies (10^{-3}/ a in decadal way to 10^{-6}/a). Table 1 shows an example of the disaggregation results. Two different methods for the disaggregation were used, the method according to NRC RG 1.165 and the method according to Bazzurro and Cornell (1999).

Table 1 Disaggregation results for distance range D1 and hazard exceedance frequency 10^{-4}/a

Spectral Frequency	Expert Opinion Combination	NRC _ Method		Bazzurro and Cornell (1999)	
	Expert Opinion Combination	M_w	D	M_w	D
5 Hz	1	5.25	5.6	5.35	1
5 Hz	2	5.75	2.4	5.65	1
5 Hz	3	5.25	4	5.05	8.6
5 Hz	4	5.25	4	5.65	1
5 Hz	5	5.75	4	5.55	1
5 Hz	6	5.25	5.6	5.95	1
5 Hz	7	6.25	5.6	5.95	1
5 Hz	8	5.75	5.6	5.95	1
5 Hz	9	5.75	5.6	5.85	1
5 Hz	10	6.25	5.6	5.45	1
5 Hz	11	5.25	7.2	5.45	9
5 Hz	12	6.75	13.6	6.45	15.4
5 Hz	13	5.25	4	6.45	11.8
5 Hz	14	5.75	7.2	5.45	9
5 Hz	15	6.25	10.4	6.35	11.8
5 Hz	16	5.25	5.6	5.45	1
5 Hz	17	5.75	2.4	5.85	1
5 Hz	18	5.25	4	5.95	1
5 Hz	19	5.75	5.6	5.85	1
5 Hz	20	5.75	5.6	5.45	1

Spectral Frequency	Expert Opinion Combination	NRC _ Method		Bazzurro and Cornell (1999)	
PGA	21	5.25	8.8	5.05	10.6
PGA	22	5.75	4	5.55	1
PGA	23	5.25	4	5.65	1
PGA	24	5.25	4	5.65	1
PGA	25	5.25	4	5.45	1
PGA	26	5.25	8.8	5.05	10.6
PGA	27	6.25	5.6	5.85	1
PGA	28	5.75	5.6	5.95	1
PGA	29	5.75	5.6	5.95	1
PGA	30	5.75	5.6	5.95	1
PGA	31	5.25	10.4	5.05	11.8
PGA	32	6.25	10.4	5.35	1
PGA	33	5.25	4	5.05	9
PGA	34	5.25	4	5.95	9
PGA	35	5.75	7.2	5.95	8.2
PGA	36	5.25	12	5.05	10.2
PGA	37	5.75	2.4	5.45	1
PGA	38	5.25	2.4	5.45	1
PGA	39	5.75	2.4	5.95	1
PGA	40	5.75	5.6	5.35	1

The results of the disaggregation were interpreted as a bivariate discrete probability distribution (magnitude and distance) of controlling earthquakes for the PEGASOS hazard at the Goesgen site.

The improved knowledge of the hazard background allowed measuring the true damaging effects of this hazard by converting the controlling earthquakes into site intensities in the EMS-98 (Gruenthal, 1998). EMS-98 intensities are statistically very well calibrated against observed damage for standardized building types. The associated vulnerability functions for the different building types allow making quantitative predictions of earthquake damage (Giovinazzi and Lagomarsino 2004).

The conversion of magnitude and distance data pairs into site intensities was based on the equations from the Earthquake Catalog of Switzerland (ECOS), Braunmiller et al (2005). The following equations were used:

1. Interception intensity

$$I_{\text{int}} = 0.096 + 1.27 M_w + 0.5 \quad \textbf{(2)}$$

2. Intensity attenuation relationship

$$\begin{aligned} &I_{site}(d) = I_{\text{int}} - fd \text{ with } f = 0.043 \text{ for } d \in (0,70)\,km \\ &\text{and } f = 0.0115 \text{ for } d \in (70,200)\,\text{km} \end{aligned} \quad \textbf{(3)}$$

The intensity attenuation relationship was intentionally based on the interception intensity and not on the epicentral intensity to account for the uncertainty related to the site conditions of the Swiss strong motion network. The additional term accounts for some possibly needed correction in site conditions (stiff soil). The intensity attenuation relationship (eqn (3)) was compared against other available intensity attenuation relationships for the region, as for example with the correlation of Segesser and Mayer-Rosa for MSK64 (ASK/SED 1977) used originally for the development of the probabilistic seismic hazard maps of Switzerland and found to be conservative. Therefore, the use of equation (3) assures a conservative representation of the epistemic uncertainty associated with intensity attenuation in Switzerland. Therefore, equations (2) and (3) were used to convert each of the scenario earthquakes obtained from the deaggregation of the PEGASOS hazard into corresponding site intensity. This allows developing a site intensity distribution for each of the hazard exceedance frequencies and each of the distance ranges used for the deaggregation of the PEGASOS hazard. Table 2 shows the main statistics of the obtained site intensity distribution in comparison with the older ASK/SED (1977) intensity attenuation model (MSK64). Fig. 4 shows as an example the intensity distribution for the hazard exceedance frequency 10-4/a and the distance range D1. The distance range D1 (the near site area dominates the PEGASOS-hazard).

Table 2 Statistical Characteristics of the site intensity distribution (EMS-98 based intensity factors)

Statistical characte-ristic	Exceedance Frequency, [1/a]	Distance Range D1		Distance Range D2		Distance Range D3	
		ECOS	ASK/SED	ECOS	ASK/SED	ECOS	ASK/SED
Mean	10^{-3}	VI.6	V.2	VI.6	V.0	VI.2	IV.3
Minimum		VI.3	IV.8	V.7	IV.0	V.0	III.0
Maximum		VII.4	VI.0	VII.6	V.9	VII.3	V.4
Mode		VI.7	V.4	VI.2	IV.9	VI.7	IV.8
Standard deviation		0.21	0.26	0.31	0.30	0.59	0.59
Mean	10^{-4}	VII.5	VII.0	VII.1	V.5	VI.6	IV.8
Minimum		VI.5	V.2	VI.2	IV.6	V.2	III.4
Maximum		VIII.6	VIII.1	VIII.4	VI.8	VIII.3	VI.6
Mode		VII.1	VI.6	VII.1	V.5	VI.7	IV.8
Standard deviation		0.50	0.79	0.61	0.61	0.70	0.69
Mean	10^{-5}	VIII.5	VIII.3	VIII.1	VI.5	VII.1	V.3
Minimum		VII.0	V.9	VI.3	IV.7	V.3	III.5
Maximum		IX.4	IX.4	IX.0	VII.4	VIII.3	VI.4
Mode		IX.4	IX.4	VIII.4	VI.8	VII.3	V.4
Standard deviation		0.69	0.77	0.64	0.64	0.58	0.58
Mean	10^{-6}	VIII.9	VIII.9	VIII.5	VI.9	VII.6	V.8
Minimum		VII.2	VI.9	VI.3	IV.7	VI.4	IV.7
Maximum		IX.8	IX.8	IX.3	VII.7	VIII.3	VI.4
Mode		IX.1	IX.1	VIII.4	VI.8	VII.3	V.4
Standard deviation		0.55	0.58	0.54	0.54	0.44	0.45

The conversion of the distribution of controlling earthquakes to site intensities allows comparing the PEGASOS hazard with the previous hazard used in the seismic PSA which was based on intensities. This comparison (for the mean hazard curves, note the old hazard derived by Basler & Hofmann was developed in MSK-intensities and then converted to average pga values; this step was reversed for the comparison) is shown in figure 5. The comparison also includes a conversion of the PEGASOS mean hazard curve in pga to intensities in MSK using the WALD correlation (Wald, 1999) and a subsequent conversion of MMI intensities to the MSK scale. The comparison clearly shows that the damaging impact of the PEGASOS hazard is lower than the damaging impact of the earlier hazard despite the increased ground motion accelerations.

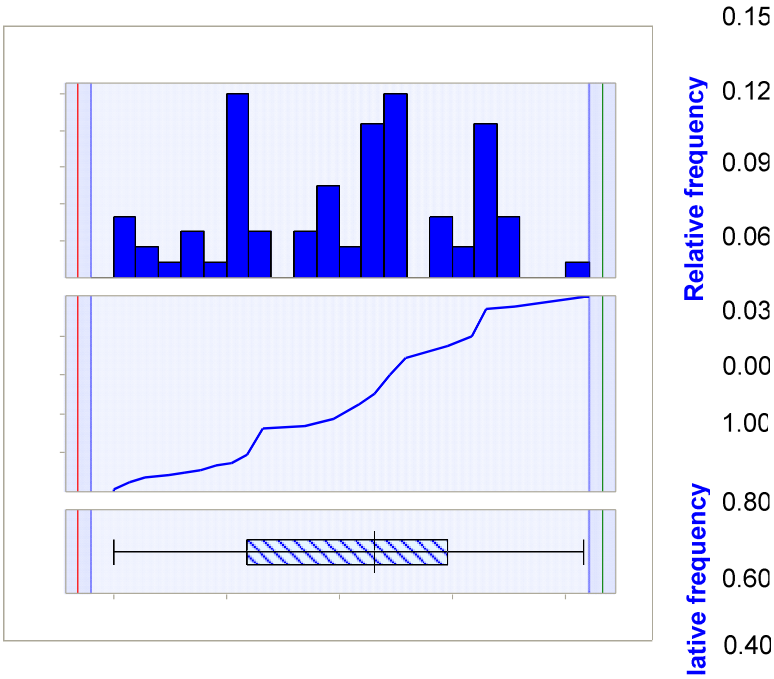

Figure 4 Site intensity distribution, distance range D1, hazard exceedance frequency 10-4/a.

Based on the comparison of the different hazards in the intensity scale it should have been expected that the core damage frequency for Goesgen (considering additionally the many seismic plant upgrades) according to the new seismic PSA should be significantly smaller than in past studies. This poses a big challenge to the method of fragility analysis. The later is acceleration based. Therefore, generally the fragility analysis will show higher failure probabilities of equipment and components with increasing acceleration despite the decreasing intensities. To deal with this phenomenon methods were developed on how to eliminate the impact of small earthquakes with no or very small damaging impact on the seismic PSA results.

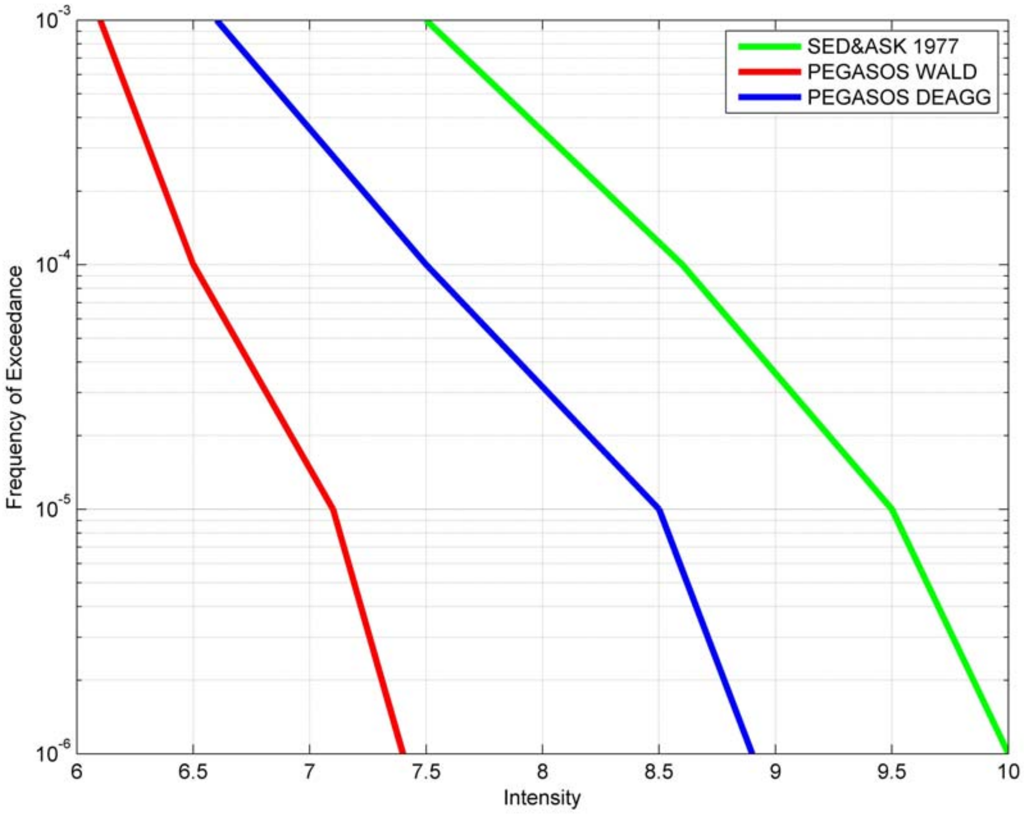

Figure 5 Comparison of PEGASOS hazard (converted into intensities) with the earlier hazard curve used for the seismic PSA of Goesgen

2.4 CAV-filtering and on the development of modern methods of fragility analysis

As a part of the update of the seismic PSA a procedure was developed for eliminating the overestimated impact of small to moderate earthquakes on the results of seismic PSA moving towards a more realistic modelling of small earthquakes as supported by empirically observed damage.

The procedure for consists of two main parts, a first one dedicated to the statistical elimination of weak non-damaging effects (CAV filtering) and a second dedicated to a more realistic description of the damaging effects of earthquakes using energy conservation principles. The procedure includes the following steps:

1. Disaggregation of the hazard in terms of probability of exceedance for different distance ranges, different spectral frequencies and for each of the single expert opinion combinations, taking different disaggregation procedures into account (US NRC RG 1.165, (NRC, 1997) and Bazzuro, 1999) as described in section 2.3. The resulting set of

scenario events (typically about 120 magnitude-distance pairs for each frequency of exceedance (called below hazard frequency) for one distance range) were interpreted as the discrete bivariate epistemic probability distribution of controlling (scenario) seismic events. This information is required both for the statistical elimination of weak non-damaging earthquakes as well as for applying an adjustment of the damaging effects of earthquakes based on energy conservation principles.

2. Selection/development of site-specific empirical correlations for the cumulative absolute velocity CAV. Analysis of influencing model parameters (e.g. focal depth) and assessment of epistemic uncertainty. According to NRC RG 1.166 (NRC, 1997) and the underlying supporting investigations, the damaging threshold of an earthquake is defined by a CAV threshold value of 0.16 gs. Empirical correlations have to be developed by nonlinear regression. The regression residuals are interpreted as spatial randomness of earthquake time histories at different locations (combines inter-event and intra-event variability).

3. Development of a Monte Carlo (bootstrap) procedure for correlated sampling of controlling events (from the developed discrete bivariate distribution) and estimation of CAV-threshold exceedance.

4. Development of a composite epistemic uncertainty distribution for the exceedance probability of the CAV threshold value, for the different distance ranges.

5. Development of a composite epistemic uncertainty distribution for the uniform hazard spectra (UHS).

6. Application of the composite distribution either for a direct adjustment of the hazard curves or in the PRA model or for the evaluation of the split fractions used to calculate the exceedance of the damaging threshold of earthquakes.

7. Development of an SSE compatible design spectrum for comparison with the existing design basis if such application is requested.

8. Evaluation of the seismic input energy submitted to a structure for each of the controlling earthquakes developed in step 1. The evaluation can be performed using empirical correlations for ARIAS intensity, CAV (as for example described in section 3) or even for strong motion duration. Alternatively, regionally validated stochastic point-source models (Campbell, 2003) can be used to develop site-specific time-histories that can be used to calculate the energy characteristics of the controlling earthquakes.

9. Adjustment of the damaging effects of earthquakes by scaling the energy content of the controlling earthquakes to a reference earthquake, either derived from the original design or selected from available databases used originally for the development of generic fragilities in terms of ground motion accelerations. This step is performed as a part of the fragility analysis.

10. Implementation of the concept of energy absorption by structures in the form of a step-shape fragility function into seismic PRA.

2.4.1 Empirical correlations for the calculation of the cumulative absolute velocity

The development of a model or of empirical equations for the calculation of the cumulative absolute velocity is a key step of the procedure for the elimination of non-damaging earthquakes. In the ideal case, the same set of data shall be used for the development of an empirical equation for CAV as was used for the development of the attenuation model of the PSHA. In the case of the PEGASOS project this was not feasible, because the original data used for the development of the different attenuation models (a total of 15 models was considered by the experts) applied in the project were not retrieved from the authors of the different models. Therefore, it was necessary to perform a detailed estimation of epistemic uncertainties associated with the use of different models or different data sets.

2.4.1.1 European Correlations

Kostov (2005) derived a set of attenuation equations for CAV for different distance ranges, using the database of European earthquake time histories. Until 2006, Kostov's work was the only publicly available information on the dependence of CAV on magnitude and distance for European conditions. Note that Kostov was not able to provide a classification of the ground characteristics for the measurement points of the European earthquake recordings used.

The equation for near-site low to moderate magnitude earthquakes is as follows:

$$\log(CAV) = -3.55 + 0.606M_s - 0.461\log(R) + P\sigma \qquad \textbf{(4)}$$

with the distance measure R based on the epicentral distance D_{epi} and the focal depth h. M_S stands for surface magnitude. The uncertainty is given as $\sigma = 0.21$, but due to the need to extrapolate to larger magnitude values, an additional epistemic component needs to be considered. Therefore, a value of **0.25** is used (corresponds to the typical values for attenuation equations for spectral accelerations).

$$R = \sqrt{\left(D_{epi}^2\right) + h^2} \qquad \textbf{(5)}$$

A second equation was developed by Kostov to calculate CAV in dependence of magnitude and distance for the more distant regional sources. This equation can be used to evaluate the exceedance probability of the critical CAV-value of 0.16 gs for the more distant seismic sources (for the associated controlling earthquakes):

$$\log(CAV) = -2.88 + 0.44M_S - 0.565\log(R) + \sigma P \qquad \textbf{(6)}$$

The associated value for σ is higher than for the equation (4) $\sigma = 0.37$.

The epicentral distance can be calculated from the Joyner-Boore-Distance , used in the PEGASOS project from the following equation (Klügel, 2005a):

$$D_{epi} = R_{JB} + \varepsilon \qquad \textbf{(7)}$$

$$\varepsilon = -0.86548 + 0.0206M^{2.8861} \qquad \textbf{(8)}$$

M here is the moment magnitude. The conversion of moment magnitude M_W to surface wave magnitude M_S is based on the equation of Ekström and Dziowonski (Ekström, 1988).

To apply Kostov's equation to the PEGASOS results, it was necessary to develop a statistical model for the distribution of focal depths in dependence of magnitude. Only the experts of SP1 provided some estimate for the focal depth of earthquakes in Switzerland, assuming a modal value of the focal depth distribution of 10 km based on observations of minor (low magnitude) earthquakes. This information was used to develop a Gamma-distribution for focal depths with magnitude-dependent mean and variation, considering the statistical dependence of focal depth on magnitude discussed by Toro (Toro, 2003) as part of the PEGASOS project. The gamma distribution obtained was used to calculate a randomized set of focal depths, corresponding to the magnitude value of the randomly selected scenario earthquake.

2.4.1.2 Development of site-specific empirical correlations for CAV from the WUS-database (EPRI 2005)

Two different sets of empirical equations were developed from the published WUS (Western United States and all over the world) database (EPRI, 2005). These published data sets are strongly classified with respect to the relevant ground characteristics in terms of the governing shear wave velocity (Vs_{30}). They contain a large amount of data from sites with similar values of shear wave velocity as the Goesgen site (in the range between 300 m/s and 500 m/s). A total of 1541 data sets were found to match the range of shear wave velocities measured for the Goesgen site (Yilmaz, 2006).

The first set of equations was developed following the regression shape suggested by Kostov, replacing the focal depth h by a free regression parameter, due to the lack of information on focal depths in the WUS database (EPRI, 2005). The following regression shape was selected for the first correlation (WUS 1):

$$\log\left(CAV\right)=b_1+b_2M+b_3\log\left(R\right)+b_4R+b_5\left(M-5.0\right)^2 \qquad \textbf{(9)}$$

Here h has the changed meaning as stated above. A similar correlation was developed for peak ground acceleration using the same data sets.

The coefficients obtained are presented in Table 3.

Table 3 Regression coefficients and standard deviation for the correlation WUS 1 (300 m/s < Vs < 500 m/s).

Parameter	b1	b2	b3	b4	b5	h	σ
log(CAV)	-5.9266	1.3811	-2.0284	0.0036717	-0.26281	17.952	0.37226
log(pga)	-3.2922	0.73851	-1.4135	0.0036421	-0.17693	11.94[1]	0.22051

A second interpretation of the data given in EPRI, 2005 selected as representative for Goesgen site conditions was developed following an idea of EPRI, 2005 using uniform duration (Bolt, 1973) as a scaling parameter. A correlation between CAV, pga and the uniform duration of an earthquake can be suggested in analogy to (Vanmarcke, 1980), where a correlation between the strong motion duration, the pga and the Arias-intensity was established. In this analogy, the uniform duration can be considered as the equivalent of the

[1] The regression resulted in a negative value for the “artificial focal depth” – the solution for this parameter is not unique because of the square root of the sum of squares in the equation. The positive branch of the solution was selected.

strong motion duration used by Vanmarcke and Lai (Vanmarcke, 1980).This analogy indicates that the following regression shapes appear to be meaningful:

$$CAV = a_1 * pga^{a_2} * d_u^{a_3} + a_4 \qquad \textbf{(10)}$$

$$\log(d_u) = c_1 + c_2 M + c_3 \log(R) + {c_5}/{(1+pga)} \qquad \textbf{(11)}$$

Here, d_u is the uniform duration. Because the calculation of CAV is defined for time windows of a length of 1s for a meaningful regression, it was necessary to consider only data sets with a uniform duration of a length of at least 1s in the regression for the uniform duration. Nevertheless, 1064 data sets were retained for the regression analysis. Table 4 and Table 5 show the coefficients for equations (10) and (11), obtained by nonlinear regression. The results of the regression confirm the almost linear dependency between CAV and the uniform duration for a fixed pga-value (a_3 is close to 1). Equations (7) and (8) are abbreviated below as WUS-correlation 2.

Table 4. **Coefficients of the alternative regression equation (7) for CAV.**

Parameter	**a1**	**a2**	**a3**	**a4**	σ
CAV	0.13435	0.34454	0.96193	0.042448	0.060404

Table 5 **Coefficients of the regression equation (8) for uniform duration.**

Parameter	**c1**	**c2**	**c3**	**c4**	**c5**	σ
d_u	-0.099174	0.32521	-0.90306	14.992	-0.014763	0.2217

Figures 6 and 7 show a comparison of the different equations for the calculation of CAV. The comparison shows that some significant differences can be observed between the different equations reflecting differences both with respect to the characteristics in recorded earthquake time-histories in Europe and the U.S.A (WUS) as well as the epistemic uncertainties associated with the selection of an appropriate equation form.

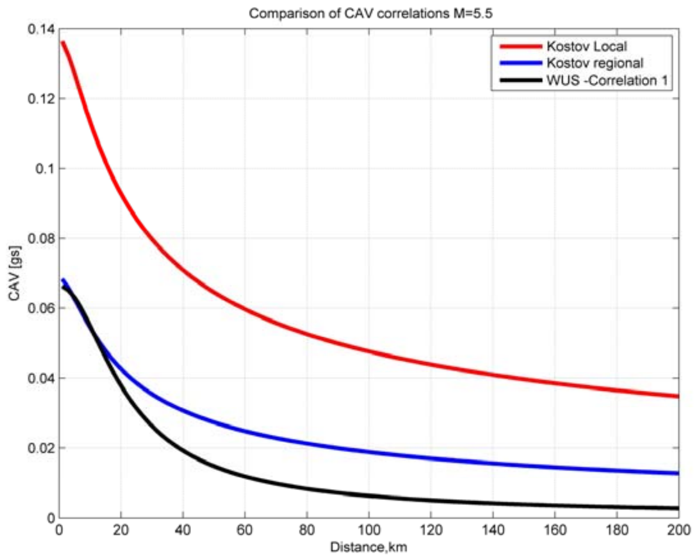

Figure 6 Comparison of Kostov's equations with the WUS-correlation 1

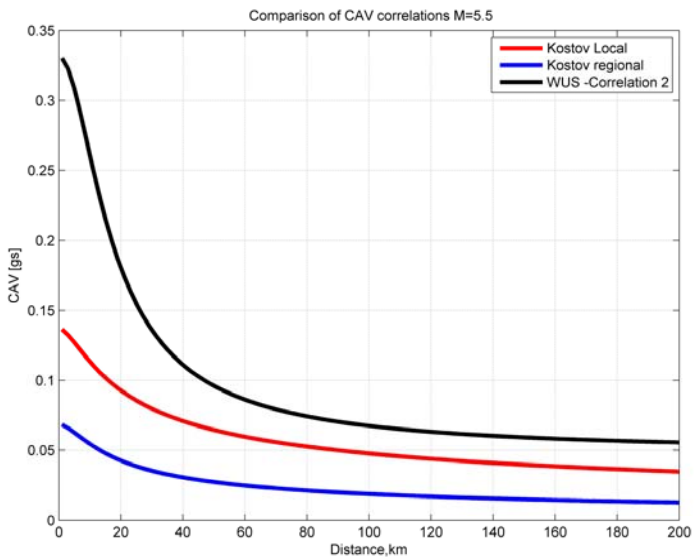

Figure 7 Comparison of Kostov's equations with the WUS-correlation 2

The equations obtained were used to calculate the probability of exceedance for the damaging threshold of earthquakes as defined in NRC RG 1.166 (CAV > 0.16 gs). For the WUS-correlation 2, an additional intermediate step is required to consider the reduction of the used data sets by eliminating short strong motion records (below 1s) statistically. Therefore, the procedure for calculating the exceedance probability of the damaging threshold had to be adjusted by weighting the exceedance of CAV > 0.16 gs with the probability that a uniform duration larger than 1s is observed.

$$P_{DL} = P_{CAV>0.16gs} P_{du \geq 1s} \qquad \textbf{(12)}$$

Here, P_{DL} is the probability of exceedance of the damaging threshold, $P_{CAV>0.16gs}$ is the probability of exceedance of CAV=0.16 gs obtained by the direct use of WUS-correlation 2 and $P_{du\geq 1s}$. Simple linear approximations in dependence of magnitude were obtained for the different distance ranges D1, D2, D3 for the probability that the uniform duration exceeds 1 s.

2.4.1.3 Development of the epistemic uncertainty distribution for the probability of exceedance of the damaging threshold of earthquakes

The exceedance probability of the damaging threshold of earthquakes was calculated for each of the developed equations, according to the bootstrap procedure discussed in section 2. Because the relative performance of the different equations may change in dependence of magnitude and distance (see example figures 4 and 5 above), the epistemic uncertainty distribution was derived in the form of a lognormal distribution assigning the calculated maximal exceedance probability of the damaging threshold for each of the hazard probabilities (abbreviation for exceedance probability of a given hazard level) to the 95% quantile of the lognormal distribution and the minimal value to the 5% quantile. This leads to a conservative stretching of the resulting epistemic uncertainty distribution towards the upper and lower tails, increasing the total amount of uncertainty considered in the model. Interpolation between the calculated values of the exceedance probability of the damaging threshold for the different hazard probabilities (which were considered in the hazard disaggregation) was performed using Hermit polynomials. This procedure was used to develop epistemic uncertainty distributions for each of the distance ranges considered (D1, D2, D3). On the basis of the developed distributions, a composite uncertainty distribution for the uniform hazard spectrum obtained from the PEGASOS results was developed by weighting the distributions for the separate distance ranges with their relative contribution to the total hazard:

$$w_i\left(H, f\right) = \frac{P_{UHS,i}\left(a_{UHS,tot}\left|\left(H, f\right)\right.\right)}{H} \qquad \textbf{(13)}$$

where $w_i\left(H, f\right)$ is the weight for the distance range *i* associated with the hazard probability *H* (e. g. for 10^{-4}/a) and the spectral acceleration *f,* and $P_{UHS,i}\left(a_{UHS,tot}\left|\left(H, f\right)\right.\right)$ is the exceedance probability of the spectral acceleration *a*, corresponding to the hazard probability *H* and the spectral frequency *f.* Figure 8 shows an example for the resulting epistemic uncertainty distribution for distance range D1 (near site sources), while figure 9 shows the resulting composite epistemic uncertainty distributions for the exceedance probability of the damaging threshold of earthquakes for different spectral frequencies (mean values) with respect to the UHS.

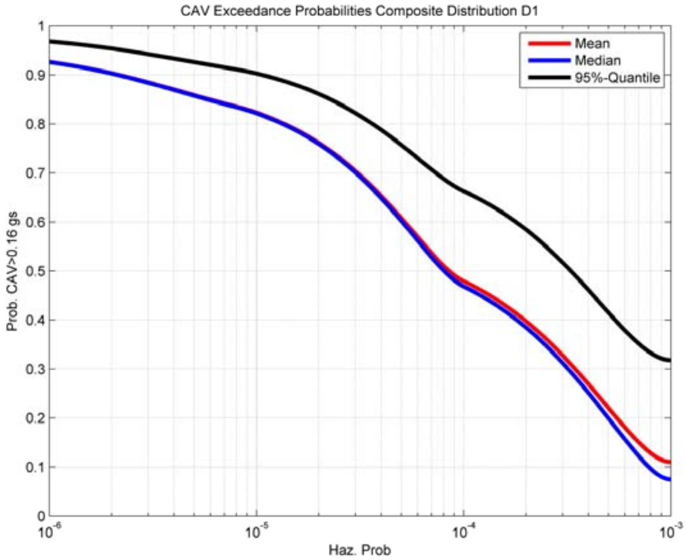

Figure 8 Composite epistemic uncertainty distribution for the probability of exceedance of the damaging threshold for distance range D1 (<16km, 3 fractiles)

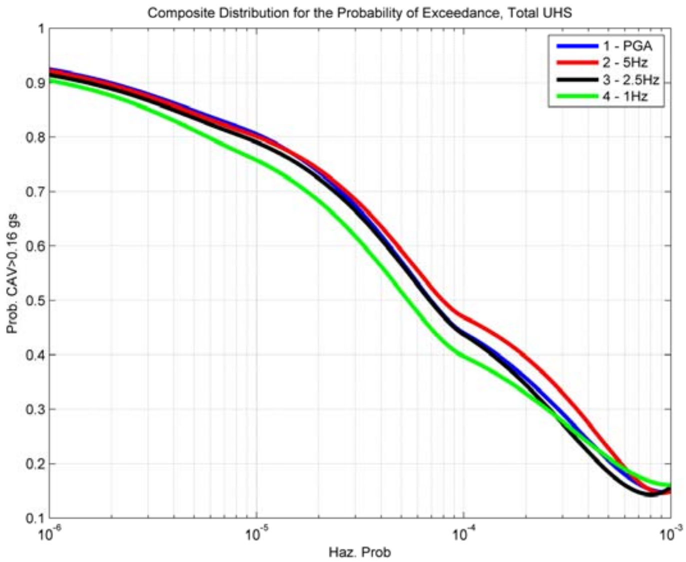

Figure 9 Composite epistemic uncertainty distribution for the probability of exceedance of the damaging threshold for the UHS

An analysis of the results presented in figure 9 shows that in the range of the frequency of exceedance of operational earthquakes (OBE) (10^{-2}/a, or for a "return period" of 475 years (2.1 10^{-3}/a) as for standard infrastructures– note the results of PSHA do not represent a temporal characteristic as is frequently misrepresented by earthquake engineers and some seismologists) nearly no damaging earthquake is to be expected.

2.4.1.4 On the treatment of small earthquakes in the traditional fragility method

The introduction of the CAV-filtering concept (EPRI, 2005, Kostov, 2005) is not sufficient to obtain realistic results in seismic risk studies for nuclear power plants as was shown in (Klügel et al, 2009a) and discussed above.

This significant difference can be explained by the circumstance that the different energy content of earthquakes of different magnitudes is not sufficiently taken into account in the standard fragility method (EPRI, 1994). Therefore, there is some need for improvement of the fragility method.

The traditional development of fragility functions for use in seismic PSA is based on the model of a double lognormal distribution for the structural capacity of structures and components. With α as the intensity parameter of an earthquake, the fragility function $F(\alpha)$ is expressed as:

$$F(\alpha) = \Phi\left[\frac{\ln\left(\alpha/C\right)}{\beta_R}\right] \qquad \textbf{(14)}$$

where β_R and $\Phi(\bullet)$ are variability of the fragility associated with random uncertainty and the cumulative standard normal distribution function, respectively. C is the seismic capacity of equipment corresponding to the level of confidence. Like intensity parameter α the anchor point of a review or design earthquake is normally used. This anchor point represents an EGA (effective ground acceleration), but it is frequently still denoted as pga, because the habit still exists of using directly an instrumental zero period acceleration as the anchor point. Other intensity parameters are possible (and frequently more suitable). The probability density function (pdf) of the seismic capacity is also lognormal:

$$f(C) = \frac{1}{\sqrt{2\pi}\beta_U C}\exp\left[-\frac{1}{2}\left\{\frac{\ln\left(C/A_m\right)}{\beta_U}\right\}^2\right] \qquad \textbf{(15)}$$

From equations (14) and (15), it can be seen that the seismic capacity is the level of the intensity parameter α (pga) at which the seismic fragility or seismic-induced failure probability equals 0.5.

Capacity *C* is obtained by evaluating the safety factor F_S, which is related to the anchor point (pga) of a review level earthquake. Variability and uncertainty β_R, β_U are usually tabulated values, which have not been changed despite the large progress achieved in earthquake engineering methods. The factor of safety is expressed as:

$$F_S = F_{SR} F_C \qquad \textbf{(16)}$$

where F_{SR} represents a set of factors associated with the seismic response to the specified acceleration and F_C is the total seismic capacity factor. The factor F_c is comparable with the total (constant) load reduction factor as used in codes like FEMA 302 or the International Building Code (ICBO, 1997). These factors account for ductility effects F_μ (in the code formulations $R(\mu,T)$), strength (overstrength in the codes) F_S and energy dissipation F_{Diss} (only considered in codes). The energy dissipation factor F_{Diss} is usually either not considered in the classical fragility formulation (set equal to 1.0) or interpreted as a small correction to the ductility factor F_μ, e.g. in EPRI, 1994, (equation. 3-34):

$$F_\mu = 1 + c_D \left(F_\mu^{'} - 1 \right) \qquad \textbf{(17)}$$

Here the factor c_D obtains a value of 1 for small magnitude earthquakes and 0.6 for long duration earthquakes. The EPRI report (EPRI. 1994) does not give any reference as to what a long duration or a small magnitude earthquake is in context of the fragility method.

This simplification was acceptable provided that:

- The seismic hazard was derived from intensities, which were converted at a subsequent step into average accelerations;
- The seismic hazard was derived as an envelope of different earthquakes with due consideration of strong motion duration, or other additional hazard parameters like peak displacements, peak velocities or ARIAS intensity;
- It was requested to assure a linear-elastic response of the structure to the design basis earthquake.

Due to the increasing use of SSHAC-type PSHA which focuses on accelerations by adding contributions from earthquakes of different energy content into a joint response spectrum (uniform hazard spectrum), this simplification is no longer justified. The main reason for this is that a uniform hazard spectrum represents the weighted combination of earthquakes of different energy potentials and thus of different damaging potentials.

Therefore, a more accurate consideration of the energy dissipation factor in the fragility method is required to avoid unrealistic results.

5 Scaling of damaging effects of different earthquakes based on energy absorption

The maximum relative displacement (or displacement ductility) is the structural parameter most widely used for evaluating the inelastic performance of structures. Nevertheless, in the recent past (in conjunction with building code developments) it has been widely recognized that the level of structural damage due to earthquakes does not depend only on maximum displacement and that the cumulative damage resulting from numerous inelastic cycles should also be taken into account. The input energy E_I is related to the cumulative damage potential of ground motions (Bertero, 1992, Fajfar, 1992, Fajfar, 1994). The energy input to an ordinary structure subjected to strong ground motion is dissipated in part by inelastic deformations (the hysteretic energy E_H) and in part by viscous damping, which represents various damping effects other than inelastic deformation. Dissipated hysteretic energy is the structural response parameter which is often correlated to cumulative damage. Fajfar and Vidic (Fajfar, 1994) proposed a procedure based on equivalent ductility factors where the reduction of ductility due to cumulative damage is controlled by the non-dimensional parameter γ, which in fact represents a normalization of dissipated hysteretic energy. They developed simple approximate formulae for determining the $\gamma\text{-spectrum}$ (Fajfar, 1994). These simplified correlations are used to develop a scaling factor for the fragility method to adjust it for considering the different energy contents of the reference design basis earthquake and any other review level earthquake (controlling earthquake from a PSHA).

The non-dimensional parameter γ, which controls the reduction of the deformation capacity of structures due to low-cycle fatigue, is defined by the formulae (Fajfar, 1994):

$$\gamma = \frac{\sqrt{\left({E_H}/{m} \right)}}{\omega D} \qquad \textbf{(18)}$$

where E_H is the dissipated hysteretic energy, *m* the mass of the system, ω the natural frequency and *D* the maximum relative displacement of the system. Equation (18) can be rewritten as follows:

$$\frac{E_H}{m} = \left(\gamma \omega D \right)^2 \qquad \textbf{(19)}$$

For a SDOF system with a bilinear force-deformation envelope, the maximum relative displacement can be computed as:

$$D = \frac{\mu Sa_e}{F_c \omega^2} \qquad \textbf{(20)}$$

where μ is the ductility factor (displacement based, maximum displacement divided by yield displacement), Sa_e is the corresponding value in the pseudo-spectral acceleration spectrum and F_c is the capacity factor from equation (16). Replacing the maximum relative displacement in equation (19) by the expression from equation (20) yields:

$$\gamma = \sqrt{\frac{E_H}{m}} \left(\frac{F_c \omega}{Sa_e \mu} \right) \qquad \textbf{(21)}$$

Equation (20) shows that the non-dimensional parameter γ for given natural frequency, ductility, a given spectral acceleration and fixed hysteretic energy (energy content of the earthquake) is directly proportional to the structural capacity factor F_c. This means that the higher the capability of a structure to absorb hysteretic energy, the higher the structural capacity factor (load reduction factor) is.

Fajfar and Vidic (Fajfar, 1994) proposed the following representation format for the non-dimensional parameter γ:

$$\gamma = z_T z_\mu z_g \qquad \textbf{\textit{(22)}}$$

Here z_T, z_μ and z_g are functions of the natural period, ductility and ground motion, respectively. This approach actually corresponds to the separation of variables approach which is characteristic for the traditional fragility analysis method. The factors z_T and z_μ are fully accounted for in the fragility analysis method. The differences in z_g are only implicitly included by the factor c_D in equation (17). Therefore, the EPRI methodology only distinguishes between cases of long strong motion duration and short strong motion duration while not giving a definition of these terms. The methodology developed by Fajfar and Vidic (Fajfar, 1994) allows accounting for the differences in the energy content of different earthquakes directly. They derived the following formula for the factor z_g:

$$z_g = \left(\frac{\int a^2 dt}{a_g v_g} \right)^{c_g} \qquad (23)$$

The integral in the numerator is the cumulative energy, which can be related to the Arias intensity AI. The factor is 0.5 in the medium period range (which is characteristic for structures of NPPs); while for the whole range of periods it is suggested to use a value of 0.4.

From the above equations it is possible to derive an additional scaling factor for the fragility analysis method, which considers the capability of structures (and components) to absorb hysteretic energy. Let us assume that a structure was designed in accordance with a nonlinear design spectrum which corresponds to a specific value of hysteretic energy. In the perfect design case we have to consider a balance of energy that means the demand – the design basis earthquake corresponds to a specific value of γ_{design}. Now let us assume that the controlling earthquake obtained as the result of a seismic hazard analysis corresponds to a completely different value of γ_{review}. Then the ratio $\gamma_{design}/\gamma_{review}$ provides a measure for the margin of the seismic design of the structure (component) of interest. If we assume that the two earthquakes considered differ only in the amount of hysteretic energy to be absorbed by the structure (component) then the ratio $\gamma_{design}/\gamma_{review}$ depends only on the different values of factor z_g in equation (22). Therefore, we arrive at an additional scaling factor (safety factor) for structures and components, which has to be considered in the fragility analysis. This factor accounts for the available seismic margin with respect to the amount of hysteretic energy, which can be sustained by a structure or components. From equations (22) and (23) it yields:

$$K_{model} = \frac{z_{g,design}}{z_{g,review}} = \left(\frac{\int a_1^2 dt}{\int a_2^2 dt} \right)^{c_g} = \left(\frac{AI_1}{AI_2} \right)^{c_g} \qquad \textbf{(24)}$$

Equation (24) represents the energy scaling relation for the structural capacity factor in fragility analysis. Because equation (24) is only applicable for nonlinear analysis, it cannot be applied for very brittle failure modes requiring a linear elastic performance of structures or components under seismic loads. Because the fragility analysis method for seismic PSA is a limit state analysis, a purely linear elastic performance of structures and components is rarely required.

A scaling relationship similar to equation (21) can be also developed on the basis of cumulative absolute velocity. In the ideal case of identical waveforms, the relation of damaging effects can simply be expressed by the ratio of the roots of the strong motion duration of the two earthquakes to be compared. The author suggests using the uniform duration (Bolt, 1973) as a measure for strong motion duration. Therefore, in the ideal case of identical waveforms (but different strong motion duration) equation (21) can be converted to:

$$K_{\text{mod}\,el} = \frac{z_{g,design}}{z_{g,review}} = \left(\frac{\int a_1^2 dt}{\int a_2^2 dt} \right)^{c_g} \approx \left(\frac{d_{u,1}}{d_{u,2}} \right)^{0.5} \qquad \textbf{(25)}$$

Traditional fragility analysis is frequently based on a scaling factor approach, where the spectral shape of the seismic demand is normalized to the spectral shape of the original design basis. In such conditions the reference pga-values (the anchor points of the normalized spectrum and of the reference design basis) earthquake may differ significantly. Under these circumstances, it is suggested to use the normalised strong motion duration in the scaling relationship of equation (25) instead of the uniform duration. The normalised strong motion duration is defined as:

$$t_{norm} = CAV \big/ pga \qquad \textbf{(26)}$$

The concept of energy absorption was extended to develop an improved shape of the fragility function for built-in components fixed to a bearing structure. As soon as a structure exhibits even only minor non-linear deformations, this leads to the absorption of energy. The nonlinear response of the structure leads to a reduction of the acceleration of the component fixed to the structure. Therefore, the probability of failure in a force-based fragility method cannot increase as long as not a new seismic failure mode, for example due to seismic interactions, is triggered. On the other hand some spectral shift of the response of the component will be observed, which is taken into account in the traditional fragility method (EPRI, 1994). This behavior can easily be reproduced by comparing the solutions of a coupled system of vibration equations for the linear case (linear response of the structure) and for the nonlinear case (nonlinear response of the structure) as is shown in Klügel (2009b). Therefore, the resulting fragility function for a component obtains a step-shape form as shown in figure 10.

The acceleration levels at which the deviation from linearity occurs and at which the capacity of the structure to absorb energy is exhausted or at which a new failure mode is triggered have to be defined in a plant (building)-specific way. In the Goesgen PRA, the onset of nonlinearities was set at about 1.2 times the acceleration level of the original operational basis earthquake (OBE) and the upper limit was set approximately to the acceleration level corresponding to a 10% probability of failure of the structure. The probability was calculated from a fragility function which combined the aleatory (random) variability and the epistemic uncertainty into one resulting probability distribution (according to the original Ang-Tang model, (Ang 1975, 1984)). This is very conservative because the epistemic uncertainty reflects lack of knowledge and therefore should only affect the statistical confidence of the distribution of the probability of failure and not the probability of failure itself (Ang, 2006).

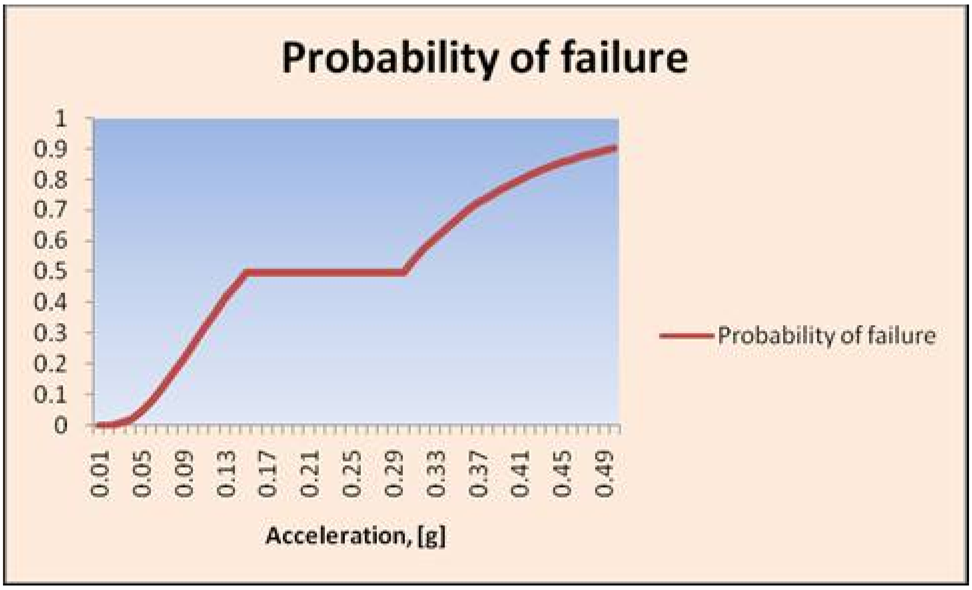

Figure 10 Fragility function for a built-in component fixed to a structure

3 Application of the procedure and Implementation of the results of PEGASOS into the seismic PSA of NPP Goesgen

In 2008 the Goesgen Nuclear Power Plant completed its regular periodic safety assessment in compliance with Swiss regulations. The re-evaluation of the seismic design and the update of the seismic PRA were important parts of the safety assessment performed by the plant. The developed procedure for the elimination of non-damaging earthquakes based on the CAV-filter was used for a comparison of the original design seismic design basis (SSE), with the hazard resulting from the PEGASOS-project (Abrahamson, 2004) after CAV-filtering. This was an important step to understand the practical implications of the results of the PEGASOS study. As a result Goesgen introduced a new seismic design basis for plant modifications, the KKG 2002 design basis spectra. These spectra had already been introduced before completion of the PEGASOS project, to provide additional safety margins for new constructions (a new wet storage spent fuel building) and for the seismic upgrade program implemented at the plant. The original seismic design basis was based on a deterministic seismic hazard analysis. The CAV-filtering, in conjunction with the consideration of increased soil parameter variability observed in recent comprehensive geotechnical investigations (Yilmaz, 2006; and in the current PEGASOS refinement project), supported the confirmation of the new KKG2002 spectra as a meaningful design basis for future plant modifications. Figure 10 shows a comparison of the design basis of Goesgen (old SSE, and the new KKG2002 design basis spectra) with a theoretical SSE derived from PEGASOS according to the NRC RG 1.165 procedures (with the exception that the SSE is based on the mean for the exceedance frequency of 10^{-4}/a according to current Swiss practice and not on the median for 10^{-5}/a) after CAV filtering and inclusion of site variability based on measured soil parameters, which leads to some reduction of the mean site amplification factor.

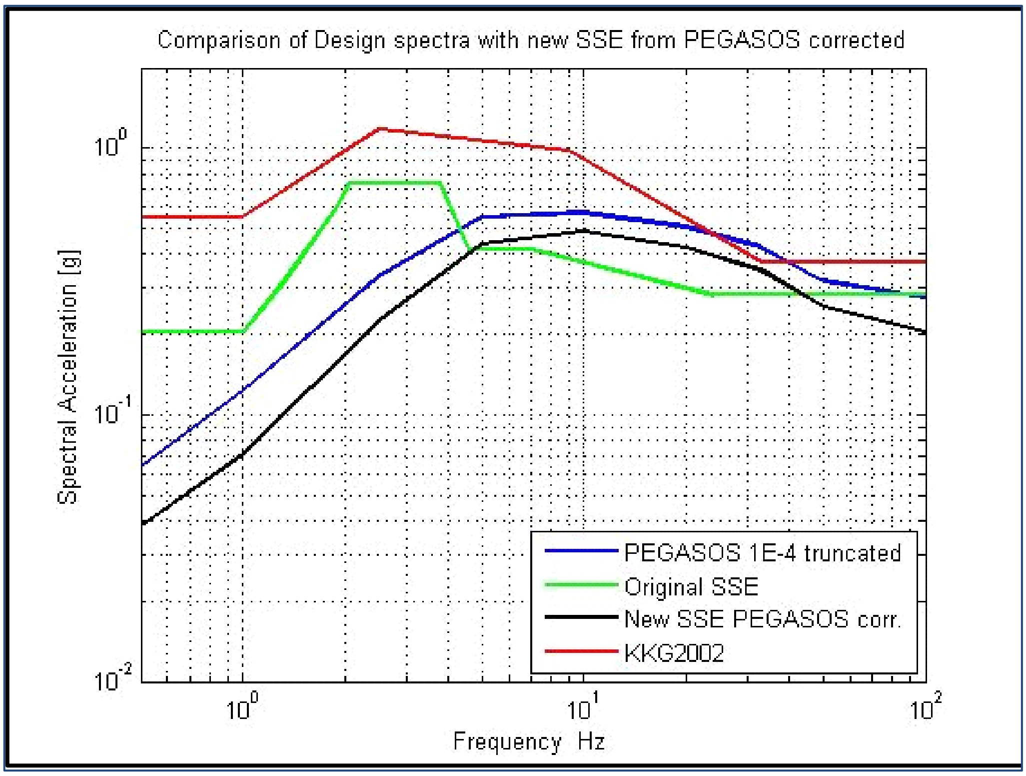

Figure 11 Comparison of deterministic SSE-design spectra with the theoretical truncated and corrected PEGASOS SSE

The comparison shows that the original deterministic design basis is in reasonable agreement with a theoretical new SSE derived from PEGASOS, while the revised design basis introduced for plant modifications in 2002 (KKG 2002) assures significant safety margins. The “energy absorption method” (scaling approach) was used in the updated fragility analysis of the plant for the seismic PRA as well as for a seismic margin analysis. The seismic margin analysis used the disaggregated hazard spectra for the exceedance frequency of 10-4/a as the review level earthquake. Due to the high level of redundancy (the availability of 3 mainly independent redundant paths for a safe shutdown of the plant) large safety margins were established. The median-centered HCLPF (High Confidence of Low Probability Failure) of the plant was found to be in the range of a pga of 0.9g. The reason for this high HCLPF value is that, according to the PEGASOS results, the seismic hazard for Goesgen NPP is driven by near-site low-to-moderate earthquakes (magnitudes below 5.5-6.0). These earthquakes have largely reduced energy content in comparison to the earthquakes which form the database used originally for the development of generic fragilities (average magnitude above 7, (Yamaguchi, 1991, Klügel, 2009a)). This effect was adequately captured by the "energy absorption" scaling method. It is worth mentioning that the HCLPF value of the plant for larger, but more distant, earthquakes is lower. But such earthquakes do also lead to lower ground motion accelerations at the site. Additionally, according to PEGASOS (Abrahamson, 2004) such earthquakes do not control the seismic hazard at the Goesgen site.

The update of the seismic PRA included a series of methodological improvements including the methodology described here:

- Incorporation of the CAV-filtering approach to identify earthquakes that are capable of causing a plant transient;
- Incorporation of the "energy absorption" scaling method for structures;
- Consideration of energy absorption by structures exhibiting minor nonlinear deformations in the fragility functions of built-in and fixed-to-the-structure components (step-shape fragility function, Klügel, 2009b)
- Improved models for correlated failures of similar redundant components under seismic loading (Klügel, 2009b)
- Improved models for the human reliability of operators (improved "Psycho-shock model", Klügel, 2007c)

The implementation of these improvements was a large effort, because it required the development of 9 different fragility cases to capture the differences of the CAV-values and the seismic energy of the associated controlling earthquakes. These fragility cases were developed from the disaggregated PEGASOS hazard. They represent the three different distance ranges (D1, D2, D3) and three different values of the frequency of exceedance (10-4/a, 10-5/a, 10-6/a). Figure 12 shows the structure of the Goesgen seismic PRA model which is a linked event tree model built in RISKMAN® (ABSG Consulting, 2009).

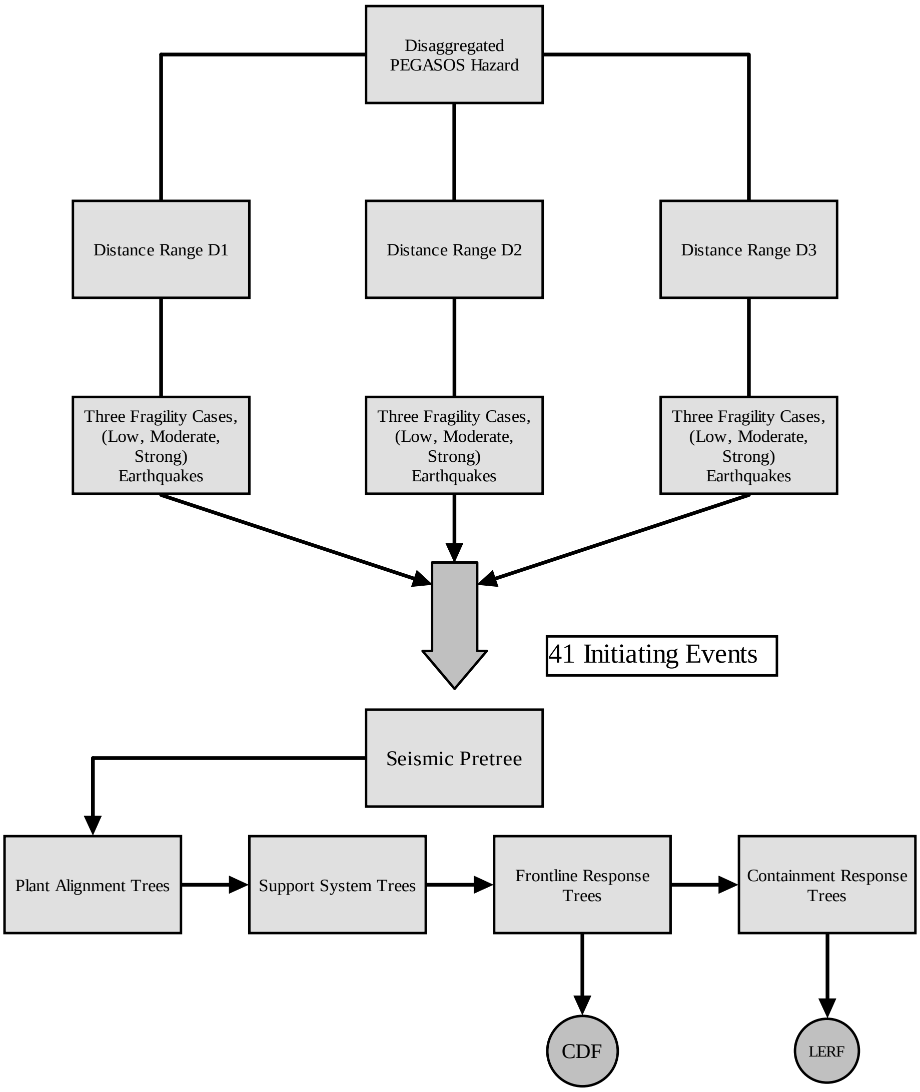

Figure 12 Structure of the Goesgen seismic PSA model

Together with the use of generally re-evaluated fragilities, these methodological improvements contributed to a significant reduction of the core damage frequency of the plant. The quantification of the new seismic PSA model confirmed the expectation that the seismic core damage frequency obtained using the PEGASOS hazard should be lower than the “old” value of the core damage frequency obtained using the original seismic hazard derived from the first probabilistic seismic hazard maps of Switzerland (ASK, 1977). The core damage frequency reduced from 1.8 x10^{-6}/a (2001- old hazard) to below 4.0 x 10^{-7}/a (2008, PEGASOS hazard). It can be concluded that the use of the suggested procedure and the additional improvements suggested for the improvement of seismic PRA lead to more realistic estimates of seismic risk which are in better compliance with historical observations with respect to damage caused by earthquakes (Klügel, 2005a).

References

Abrahamson, N. A., Coppersmith, K.J., Koller, M., Roth, P., Sprecher, C., Toro, G.R., and Youngs, R., 2004. Probabilistic Seismic Hazard Analysis for Swiss Nuclear Power Plant Sites (PEGASOS Project), Vol. 1 to 6, NAGRA.

ABSG Consulting, 2009. RISKMAN® for Windows Version 11.2, User Manual, ABSG Consulting, Irvine (CA).

Ang, A. and Tang, W., 1975. Probability Concepts in Engineering Planning and Design, Vol. I. John Wiley, New York.

Ang, A. and Tang, W., 1984. Probability Concepts in Engineering Planning and Design, Vol. II. John Wiley, New York.

Ang A. and Tang, W., 2006. Probability Concepts in Engineering. Emphasis on Applications to Civil and Environmental Engineering, 2nd edition, Wiley, New York.

Arias, A., 1970. A measure of earthquake intensity. In R.J. Hansen (Eds.): Seismic Design for Nuclear Power Plants, MIT Press, Cambridge, Massachusetts.

ASK (Abteilung für die Sicherheit der Kernanlagen, Basler& Hofmann, Schweizerischer Erdbebendienst), 1977. Erdbebenrisikokarten der Schweiz.

Ayyub, B.M. and Klir, G.J., 2006. Uncertainty Modeling and Analysis in Engineering and the Sciences, Chapman &Hall/CRC, Boca Raton, London, New York, 378 p.

Bazzuro, P. and Cornell, C.A., 1999. Disaggregation of Seismic Hazard, Bulletin of the Seismological Society of America, 82, pp. 501-520.

Bertero, V.V. and Uang, C.M., 1992. Issues and Future Directions in the Use of an Energy Approach for Seismic-Resistant Design of Structures; In Nonlinear Seismic Analysis and Design of Reinforced Concrete Buildings, Ed. P. Fajfar and H. Krawinkler, 3-22.

Bolt, B.A.,1973. Duration of Strong Ground Motion, Proc. Fifth World Conf. Earth Eng., Rome, 1304-1307.

Braunmiller, J., Deichmann, N., Giardini, D., Wiesmer S., and the SED Magnitude Working Group, 2005. Homogeneous Moment-Magnitude Calibration in Switzerland, Bulletin of the Seismological Society of America, 95(1), pp. 58-74.

Campbell, K.W., 2003. Prediction of Strong Ground Motion Using the Hybrid Empirical Method and Its use in the development of Ground- Motion (Attenuation) Relations in Eastern North America.

Cooke, R.M., 1991. Experts in Uncertainty. Opinion and Subjective Probability in Science. Oxford University Press, Oxford.

Cooke, R.M., Goossens, L.L.H.J., 2008. TU Delft Expert Judgement Database, Reliability Engineering & System Safety, 93, pp. 657-674.

Ekström, G. and Dziewonski, A.M., 1988. Evidence of Bias in Estimation of Earthquake Size. Nature, 332, pp.319-323.

Electric Power Research Institute (EPRI), 1994. Methodology for Developing Seismic Fragilities, TR-103959.

Electric Power Research Institute (EPRI), Program on Technology Innovation: Use of CAV in Determining Effects of Small Magnitude Earthquakes on Seismic Hazard Analyses, TI-1012965, Dec 2005.

Fajfar, P., 1992. Equivalent Ductility Factors, Taking into account low-cycle fatigue. Earthquake Engineering and Structural Dynamics, 21, 837-848.

Fajfar, P. and Vidic, T., 1994. Consistent Inelastic Design Spectra: Hysteretic and Input Energy, Earthquake Engineering and Structural Dynamics, 23, 523-537.

FEMA 302 – NEHRP Recommended Provisions for Seismic Regulations for New Buildings and Other Structures – Part 1- Provisions, NEHRP, 1997.

Giovinazzi, S. and Lagomarsino, S., 2004. A Macroseismic Method for the Vulnerability Assessment of Buildings. 13th World Conference on Earthquake Engineering, Vancouver, B.C., Canada, August 1-6, 2004, Paper No. 896.

Grünthal, G., 1998. European Macroseismic Scale 1998. Cahiers du Centre Européen de Géodynamique et de Séismologie, Vol. 15, 100p.

International Conference of Building Officials (ICBO), 1997. Uniform Building Code 1997 Edition, ICBO, Whittier, CA.

Klügel, J.-U., 2005a. Problems in the Application of the SSHAC Probability Method for Assessing Earthquake Hazards at Swiss Nuclear Power Plants. Engineering Geology, 78, pp. 285-307.

Klügel, J.-U., 2005b. Reply to the Comment on J.U. Klügel's "Problems in the Application of the SSHAC Probability Method for Assessing Earthquake Hazards at Swiss Nuclear

Power Plants“, in Engineering Geology, Vol. 78, pp. 285-307, by Budnitz, by J.U-Klügel, Engineering Geology, 82, pp. 79-85.

Klügel, J.-U., 2005c. Reply to the Comment on J.U. Klügel’s “Problems in the Application of the SSHAC Probability Method for Assessing Earthquake Hazards at Swiss Nuclear Power Plants“, in Engineering Geology, Vol. 78, pp. 285-307, by Musson, Engineering Geology, 82, pp. 56-65.

Klügel, J.-U., 2007a. Error Inflation in Probabilistic Seismic Hazard Analysis, Engineering Geology, 90, pp. 186-192.

Klügel, J.-U., 2007b. Comment on “Why Do Modern Probabilistic Seismic-Hazard Analyses Often Lead to Increased Hazard Estimates” by Julian J. Bommer and Norman A. Abrahamson or “How not to Treat Uncertainties in PSHA”, Bulletin of the Seismological Society of America, 97 (6), pp. 2198-2207.

Klügel, J.-U., 2007c., An Improved Methodology for the Evaluation of Human Error Probabilities in a seismic PSA, SMIRT 19, Toronto August 12th-17th , paper #1143.

Klügel, J.-U., 2008a. Seismic Hazard Analysis - Quo vadis? Earth-Science Reviews, 88, pp. 1-32.

Klügel, J.-U., 2008b. PSÜ 2008: Überprüfung der Erdbebenauslegung des KKG, Kernkraftwerk Goesgen, BER-D-31030., 92p.

Klügel, J.-U., Rao, S.B., Mikschl, T. and the members of the Goesgen PSA team. 2008c. GPSA 2009 Goesgen Probabilistic Safety Assessment, ABS Consulting, R-1699596-1751, 9 modules.

Klügel, J.-U., Attinger, Richard, Rao, S, B., and Vaidya, Nish, 2009a. Adjusting the Fragility Analysis Method to the Seismic Hazard Input, Part I: The Intensity-based Method, International Conference on Structural Mechanics in Reactor Technology, SMiRT 20 , paper #1567, Espoo, Finland.

Klügel, J.-U., Attinger, Richard, Rao, S, B., and Vaidya, Nish, 2009b. Adjusting the Fragility Analysis Method to the Seismic Hazard Input, Part II: The Energy Absorption Method, International Conference on Structural Mechanics in Reactor Technology, SMiRT 20 , paper #1568, Espoo, Finland.

Klügel, J.-U., 2009. On the treatment of Dependency of Seismically Induced Component Failures in Seismic PRA, International Conference on Structural Mechanics in Reactor Technology, SMiRT 20 , SMIRT 20 .#1581, Espoo, Finland

Kostov, M. K., 2005. Site Specific Estimation of Cumulative Absolute Velocity, in Proceedings of 18th International Conference on Structural Mechanics in Reactor Technology, Beijing, August 7 – 12, 2005.

Labbè, P., 2007, PSHA results vs historical seismicity, Experience on the Implementation of the Outputs from Probabilistic Seismic Hazard Analyses in France and Switzerland, Workshop Beznau, Switzerland.

Miller, A.C. and Rice, T.R., 1983. Discrete approximations of probability distributions. Management Science, 29, pp. 352-362.

Newmark, N.M. and Hall, W.J., 1982. Earthquake Spectra and Design, EERI Monograph Series, Earthquake Engineering Research Institute, Oakland, CA.

NRC RG 1.166, 1997. Pre-Earthquake Planning and Immediate Nuclear Power Plant Operator Postearthquake Actions, RG 1.166.

NRC, 1997. Identification and Characterization of Seismic Sources and Determination of Safe Shutdown Earthquake Ground Motion. RG 1.165.

Senior Seismic Hazard Analysis Committee (SSHAC), 1997. Recommendations for Probabilistic Seismic Hazard Analysis: Guidance on Uncertainty and Use of Experts. NU-REG/CR-6372.

Toro, G. R., 2003. Technical Note to SP1 Experts on the Treatment of Hypocentral Depths and Rupture-length Effects for Area Sources in the FRISK88MP Software, 19.5.2003.

Vanmarcke, E.H. and Lai, S.S.P., 1980. Strong Motion Duration and RMS Amplitude of Earthquake Records, Bulletin of the Seismological Society of America, Vol. 70, No. 4, pp.1293-1307.

Vidic, T., Fajfar, P., and Fischinger, M., 1994. Consistent Inelastic Design Spectra: Strength and Displacement, Earthquake Engineering and Structural Dynamics, 23, 507-521.

Yamaguchi, A., Campbell R.D. and Ravindra, M.K. 1991., Bayesian Methodology for Generic Seismic Fragility Evaluation of Components in Nuclear Power Plants, Structural Mechanics in Reactor Technology 11, Tokyo, paper Mo4/3, August 1991.

Yilmaz, O., 2006. Report on Shallow Seismic Investigation at NPP Goesgen Site, Switzerland., Anatolian Geophysical. Kaplan, S., Garrick, B.J. 1981. On the Quantitative Definition of Risk, Risk Analysis, 1: 11-27,